Controlling Symmetry Breaking Charge Transfer in BODIPY pairs

Laura Estergreen[1†], Austin R. Mencke[1], Daniel E. Cotton[2], Nadezhda V. Korovina[3††], Josef Michl[3], Sean T. Roberts[2], Mark E. Thompson[1]*, Stephen E. Bradforth[1]*

1. Department of Chemistry, University of Southern California, Los Angeles CA 90089.
2. Department of Chemistry, University of Texas at Austin, Austin TX 78712
3. Department of Chemistry, University of Colorado Boulder, Boulder, CO 80309

[†] Current address: Department of Chemistry, University of Texas at Austin, Austin, TX 78712
[††] Current address: Department of Chemistry, California State University, Chico, Chico, CA 95929

*Corresponding Authors
Mark Thompson: met@usc.edu
Stephen Bradforth: stephen.bradforth@usc.edu

Conspectus:

Symmetry breaking charge transfer (SBCT) is a process in which a pair of identical chromophores absorb a photon and use its energy to transfer an electron from one chromophore to the other, breaking the symmetry of the chromophore pair. This excited state phenomenon is observed in photosynthetic organisms where it enables efficient formation of separated charges that ultimately catalyze biosynthesis. SBCT has also been proposed as a means for developing photovoltaics and photocatalytic systems that operate with minimal energy loss. It is known that SBCT in both biological and artificial systems is in part made possible by the local environment in which it occurs, which can move to stabilize the asymmetric SBCT state. However, how environmental degrees of freedom act in concert with steric and structural constraints placed on a chromophore pair to dictate its ability to generate long-lived charge pairs via SBCT remain open topics of investigation.

In this work we compare a broad series of dipyrrin dimers that are linked by distinct bridging groups to discern how the spatial separation and mutual orientation of linked chromophores and the structural flexibility of their linker each impact SBCT efficiency. Across this material set, we observe a general trend that SBCT is accelerated as the spatial separation between dimer chromophores decreases, consistent with the expectation that the electronic coupling between these units varies exponentially with their separation. However, one key observation is that the rate of charge recombination following SBCT was found to slow with decreasing interchromophore separation, rather than speed up. This stems from an enhancement of the dimers' structural rigidity due to increasing steric repulsion as the length of their linker shrinks. This rigidity further inhibits charge recombination in systems where symmetry has already enforced zero HOMO-LUMO overlap. Additionally, for the forward transfer the active torsion is

shown to increase LUMO-LUMO coupling, allowing for faster SBCT within bridging groups.

By understanding trends for how rates of SBCT and charge recombination depend on a dimer's internal structure and their environment, we identify design guidelines for creating artificial systems for driving sustained light-induced charge separation. Such systems can find application in solar energy technologies and photocatalytic applications but can serve as a model for light-induced charge separation in biological systems.

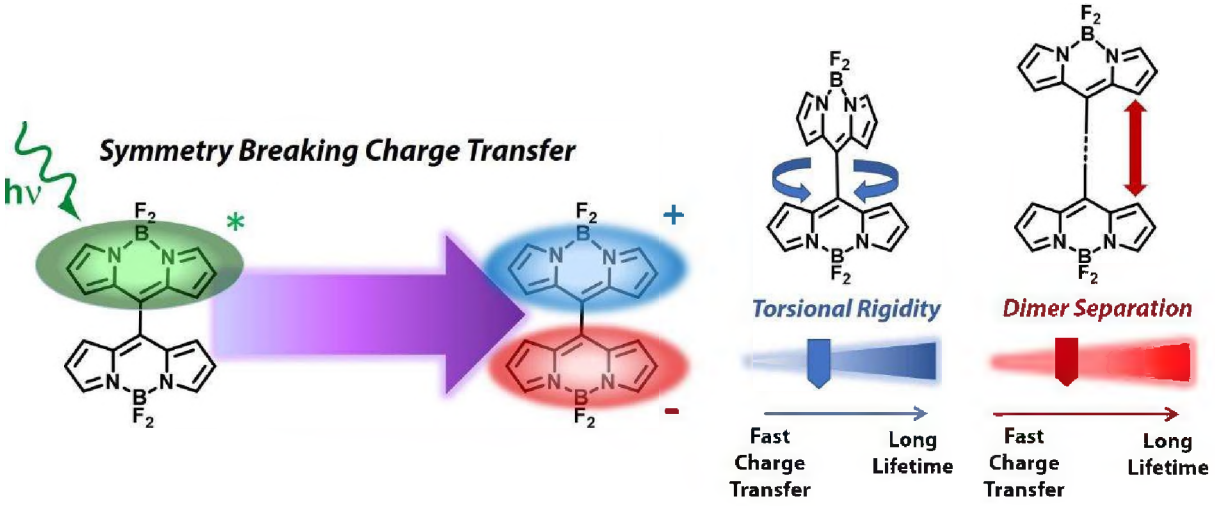

KEY REFERENCES

- Whited, M. T.; Patel, N. M.; Roberts, S. T.; Allen, K.; Djurovich, P. I.; Bradforth, S. E.; Thompson, M. E. Symmetry-Breaking Intramolecular Charge Transfer in the Excited State of Meso-Linked BODIPY Dyads. *Chem Commun* **2011**, *48* (2), 284–286.[1] *Characterization of a directly-linked and a phenylene bridged BODIPY dimer and analysis of their relative SBCT rates. Steady-state photophysical and electrochemical characterizations are coupled to solvent-dependent transient absorption to discuss mechanisms for formation and decay from the SBCT state.*
- Trinh, C.; Kirlikovali, K.; Das, S.; Ener, M. E.; Gray, H. B.; Djurovich, P.; Bradforth, S. E.; Thompson, M. E. Symmetry-Breaking Charge Transfer of Visible Light Absorbing Systems: Zinc Dipyrrins. *J Phys Chem C* **2014**, *118* (38), 21834–21845.[2] *SBCT within a series of zinc dipyrrinato dimers were studied as a function of their solvent-dependent photophysical steady-state and transient properties. Spin-triplet excited states are found to be a decay path from the SBCT state.*
- Kellogg, M.; Akil, A.; Ravinson, D. S. M.; Estergreen, L.; Bradforth, S. E.; Thompson, M. E. Symmetry Breaking Charge Transfer as a Means to Study Electron Transfer with No Driving Force. *Faraday Discuss* **2019**, *216* (0), 379–394.[3] *SBCT in a zinc dipyrrinato dimer system was found to occur with no driving force in a binary solvent mixture. Additionally, SBCT within a zinc dipyrrinato dimer and a directly-linked BODIPY dimer was compared using transient absorption and time-dependent DFT calculations. It was found that the charged zinc moves toward the anion dipyrrin in the SBCT state, giving a lower dipole moment of its SBCT state relative to the BODIPY dimer.*

Introduction

In nature, several organisms employ solar energy toward biosynthesis. Photosystem II (PS II) in plants[4–6] and the photosystems of *Rhodobacter sphaeroides*[5,7–10] and *Rhodopseudomonas viridis*[10,11] are some of the most studied photosynthetic systems for converting solar energy into chemical fuels. These systems contain light-harvesting centers (LHCs) and reaction centers (RCs) that work in tandem to synthesize adenosine triphosphate (ATP)[4] from light-generated excitations by using them to drive unidirectional charge transfer[4,5]. Within PS II's RC resides a chlorophyll dimer surrounded by a pair of accessory chlorophylls and pheophytins. This multiplex is held in a C_2 symmetry by the protein frame, though only one side is active in electron transfer[4]. The RC's central dimer is typically referred to as a 'special pair' as the two cofacial chlorophylls are spatially arranged in a manner that allows them to use energy delivered to the RC from the LHC to drive charge separation.

Generation of ATP by RCs is incredibly efficient. In plants, this process occurs with 90% thermodynamic efficiency[4] while bacteria achieve 100% quantum efficiency for charge transfer per photon absorbed[12,13]. Their impressive ability to separate charge suggests photosynthetic RCs can serve as a functional model for artificial systems that harvest light to produce solar fuels. A RC's special pair uses its environmental asymmetry to enable light-driven charge transfer, breaking the pair's symmetry. As this charge transfer produces an electron and hole sufficiently uncoupled to behave independently, it is referred to as symmetry breaking charge separation (SBCS).

Synthetic approaches have been used to explore SBCS to further our understanding of this process and advance our ability to create systems that readily separate charge[12,14–18]. Several asymmetric donor-acceptor (D-A) systems have been made where electron and hole transfer are

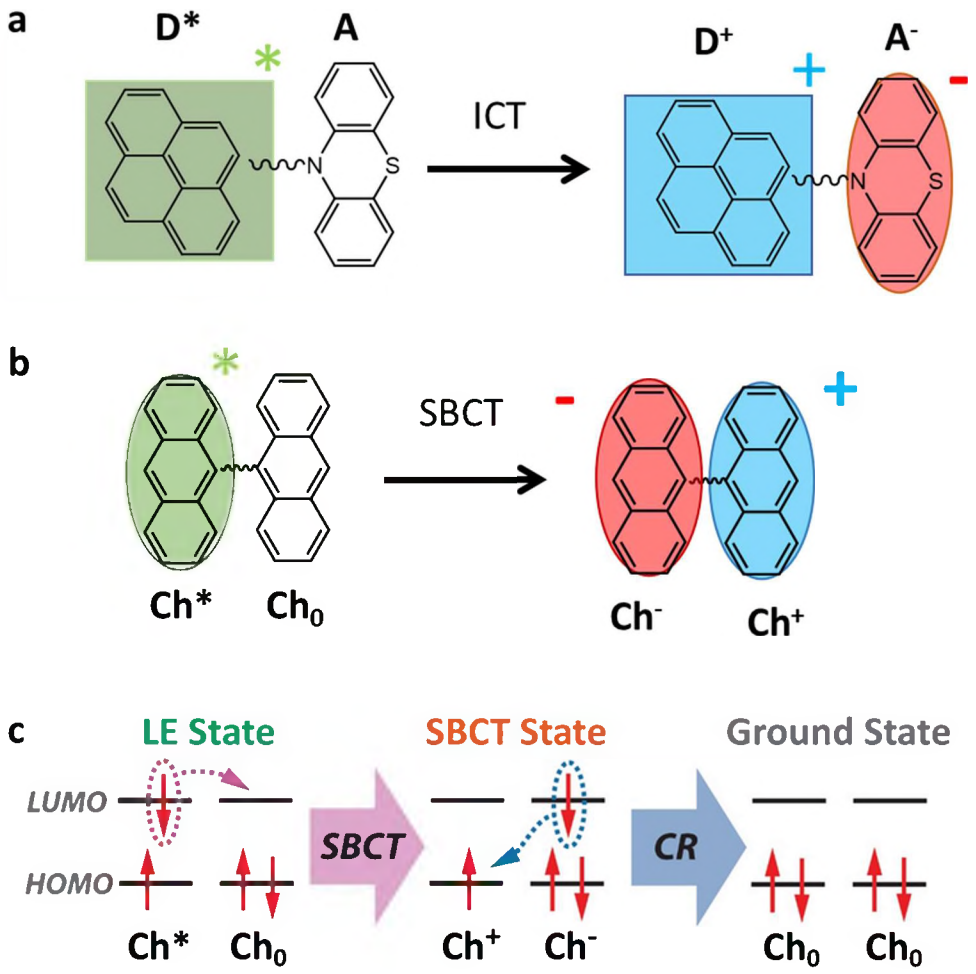

Figure 1: (a) Intramolecular charge transfer (ICT), where the "donor" chromophore is initially excited (D*) followed by electron transfer to an acceptor (A) leaving D^+. (b) Symmetry breaking charge transfer (SBCT) between a set of identical chromophores (Ch) such as anthracene. In weakly coupled dimers, light absorption generally excites one member of the dimer pair (Ch*), producing a localized excited state (LE) that undergoes SBCT to form a cation (Ch^+) and anion (Ch^-). (c) Cartoon highlighting the exchange of electrons between orbitals needed for SBCT and CR within a minimal four-electron model. While SBCT driven by electron transfer involves LUMO-LUMO spatial overlap, CR is instead dependent on HOMO-LUMO overlap, suggesting bridge design can be used to enhance the former and suppress the latter. We note that a complementary pathway leading to the SBCT state can be achieved via hole transfer from Ch* to Ch_0, which depends on HOMO-HOMO overlap.

energetically dictated to be unidirectional (D-A + hν → $^+$D-A$^-$)[14,19–24]. Such intramolecular charge transfer (ICT) systems generally employ differences in redox properties of the electron donor and acceptor to conduct electrons and holes along distinct, unidirectional paths (**Figure 1a**).

However, ICT has also been achieved in entirely symmetric molecular dimers (**Figure 1b**).

Upon absorption of a photon, weakly coupled dimers form an excited state which dynamically localizes on one chromophore (Ch) of the molecular pair, rapidly producing a localized excited state (LE), **Figure 1c**, rather than one that extends over the full dimer. Isolated, these systems lack a mechanism for charge separation as there is no means to stabilize the separated anion and cation. Rather, fluctuations in the local solvent environment surrounding the dimer create an asymmetry in its two units that can drive separation and stabilize the resulting radical anion (Ch^-) and radical cation (Ch^+) as depicted in **Figure 1c**. In this sense, these symmetric systems are not unlike the special pair, wherein the protein scaffold holding the pair provides an asymmetric energy gradient that separates charge. We refer to this type of ICT in symmetric dimers as symmetry breaking charge transfer (SBCT). Unlike the special pair, if there is no medium to collect the resultant charges, they will recombine (CR) back to the ground state. The SBCT state in **Figure 1c** is shown as a singlet, but its triplet form is close in energy, facilitating intersystem crossing (ISC).[2,25–27] In some cases the triplet SBCT state can relax to a Ch localized triplet (*vide infra*).

While related, experimentalists have used the emission properties of the charge transfer state produced by a dimer to distinguish SBCT and SBCS.[21,28] SBCT typically yields an emissive charge transfer state while SBCS often produces a charge-separated state that decays only non-radiatively. This distinction partially reflects the degree of coupling between the spatially separated electron and hole. SBCS generally produces electrons and holes that are fully decoupled and behave independently while SBCT produces electron-hole pairs that remain weakly coupled and can be thought of as Wannier-Mott or charge transfer excitons. Herein, SBCS will be treated throughout this review as a type of SBCT, where the resulting charges are in the "decoupled" limit.

Here, we explore how the formation rate and longevity of SBCT states created between dipyrrin dimers is dictated by their structure. Though dimer environment plays a large role in SBCT as it can tune the energy of the initial LE and final SBCT states, dimer intramolecular structure can manipulate activation barriers that affect mechanistic pathways toward SBCT as well as the decay of the SBCT state via charge recombination. As depicted in **Figure 1c**, for instance, we see that charge transfer requires spatial overlap between the valence orbitals of the coupled chromophores (either LUMO-LUMO or HOMO-HOMO overlap). Additionally, charge recombination, which may impact the lifetime of the SBCT state, is also dependent on orbital overlap of the resultant cation and anion (HOMO-LUMO overlap). This implies that the spatial separation and relative orientation of dimers engaging in SBCT play significant roles in dictating the rate and longevity of charge separation.

We note coupled dimers similar to those we investigate here have shown great promise as systems for achieving intramolecular singlet fission[29–34,35,35] As electronic coupling mediated by charge transfer often plays a key role in enabling singlet fission, we anticipate the principles we highlight below for creating systems that exhibit prolonged charge separation via SBCT can be extended to generate materials that efficiently produce triplet exciton pairs for applications in energy conversion and quantum information.

A Brief Review of SBCT in 9,9'-Bianthryl

Among compounds that undergo SBCT, 9,9'-binathryl (BA) is perhaps the most studied. Emission spectra of BA show a strong solvent dependence indicative of ICT [22,36–38] that can be viewed via femtosecond transient absorption (TA)[22,37] and time-resolved photoluminescence spectroscopy[38]. In nonpolar solvents, emission spectra of BA are broadened and do not resemble their corresponding absorption lineshapes. This broadening has been attributed to torsion about the

dihedral angle on the bridge between the two anthracene planes,[22,36] a motion observed using 10 fs pulses[39]. While anthracene lacks a static dipole moment in the S_1 state, flash-photolysis time-resolved microwave conductivity experiments indicate BA develops a significant static dipole moment in its excited state, even when it is dissolved in nonpolar solvents.[40] BA's dipole in its LE state has been attributed to it containing charge resonance contributions (Ch^+-Ch^- and Ch^--Ch^+) whose degeneracy is lifted by intramolecular torsion and solvent fluctuations, producing a net dipole moment in excited BA[40]. Fluorescence upconversion experiments coupled to molecular dynamics (MD) simulations have also explored the nature of these stabilizing solvent fluctuations, showing that solvent molecules modulate SBCT by reorienting to induce local electric fields.[41] Once formed, the dipole moment associated with the SBCT state stabilizes these solvent arrangements, making reformation of the LE state unfavorable.

It has been shown that BA's torsional angle is an active coordinate toward SBCT,[22,39,41] as illustrated in **Figure 2**, which shows a cartoon highlighting how the energy of the LE and SBCT states change as a function of this angle. When placed in its LE state, BA favors a twisted structure with minima at ~60° and 120°.[22,39,41] While initial work suggested that the SBCT state adopted similar minima,[21,29] recent work by Lee et. al. using quantum-mechanical molecular dynamic simulations showed that the SBCT state instead adopts a torsional angle of 90° with a large distribution of about ±10°, which matches BA's ground state where explicit MeCN molecules were allowed to rotate, driving SBCT.[41] These differences in potential energy minima suggest torsional motion is needed to transition the LE state to the SBCT state in concert with solvent reorientation.

Moreover, near-infrared pump-probe anisotropy experiments[42] coupled to time-resolved microwave conductivity experiments[40] suggest formation of a unique excited state prior to SBCT

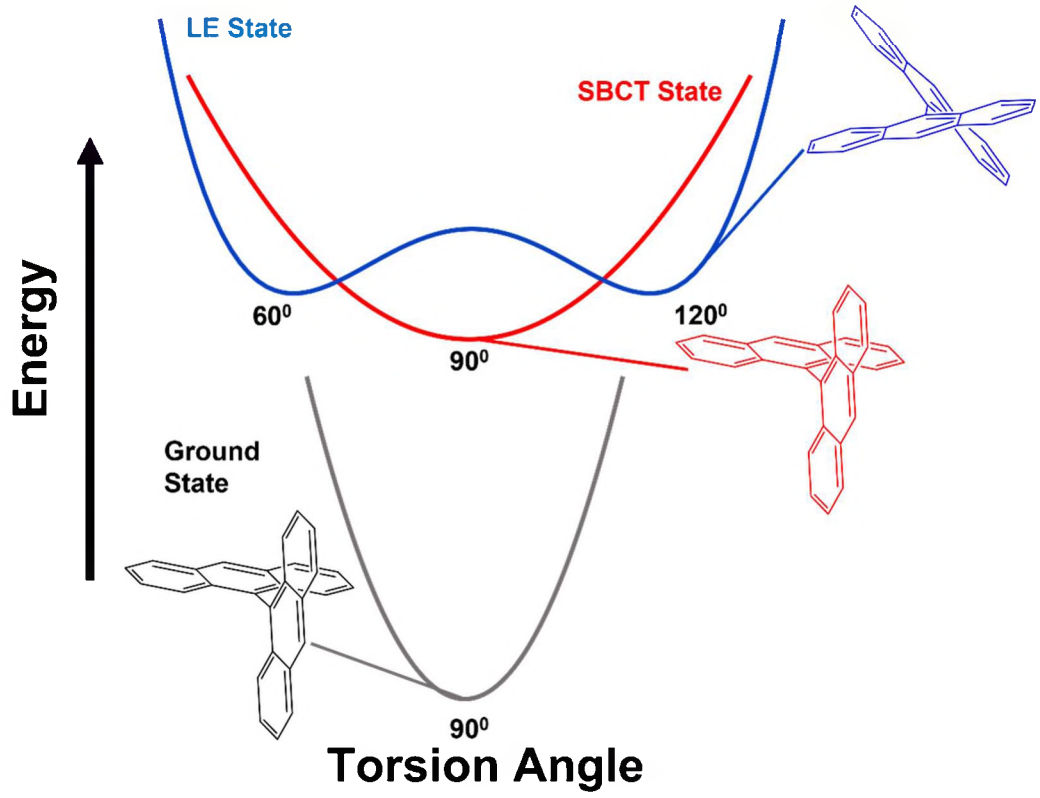

Figure 2: Cartoon illustration of potential energy surfaces for the LE state (blue) and SBCT state (red) of BA. A representative PCT state surface is not shown here as calculations are not available.

that is distinct from the LE state. In nonpolar solvents, BA does not evolve beyond population of this intermediate state while in polar media SBCT continues to completion[42]. This intermediate has been denoted as a partial charge transfer (PCT) state and is comprised of a charge transfer state that is strongly coupled to the LE state where the transition dipole moment was found to be along BA's *meso* bridge. PCT formation is proposed to be driven by a transient, unequal interaction of BA's anthracene moieties with their solvent environment.[42,43] Thus, the proposed mechanism for SBCT in BA in a solvating environment is formation of an LE state that evolves to a PCT state from which complete charge transfer occurs (LE □ PCT □ SBCT)[42,44]. Taken together, these findings highlight that a solvent can play an active role in SBCT by stabilizing key charge-separated intermediates as a dimer evolves in its structure over time. Several other systems have been explored for the application of SBCT including perylene[28,45,46] and perylene diimide[17] dimers

as well as certain Donor-Acceptor-Donor[15] (or Acceptor-Donor-Acceptor[47]) systems. However, BA is a historical model system for SBCT and is the most relatable system to aid in explaining the observations described in the following sections.

SBCT in Dipyrrin Dimers

Boron dipyrromethene (BODIPY) dyes are known for their tunability, high molar absorptivity, long-lived excited states[48], and quasi-reversible redox potentials[49], making them excellent candidates for light-harvesting applications that require SBCT. Prior work from our groups have shown dimers structurally similar to BA, prepared with either DIPYR (borondifluoro dipyridylmethene)[50] or BODIPY,[1,3] undergo either PCT or full SBCT depending on their structure and local environment. In these dimers the *meso*-positions of the chromophores can be bridged by a single bond as in *bis*-DIPYR and **m_nB** or by a phenylene spacer as in **m_nPh** (**Scheme 1**). Importantly, even minor structural changes greatly impact the ability of a BODIPY pair to interconvert between LE and SBCT states. This provides a chemical handle by which rates for SBCT, CR, and formation of key states such as triplets,[2,27] can be manipulated to meet the demands of a given application. For example, torsion of the chromophores about their connecting bridge can be sterically constrained to extend the lifetime of SBCT states (*vide infra*). Likewise, through-bond coupling, which is dependent on orbital overlap and impacts the rate of SBCT, can be adjusted through linking bridge design[1] or even outright eliminated via use of simple ions, such as Zn^{2+}, as linkers[2,3,51] (**zDIP**, **Scheme 1**).

Scheme 1. Materials investigated in this report.

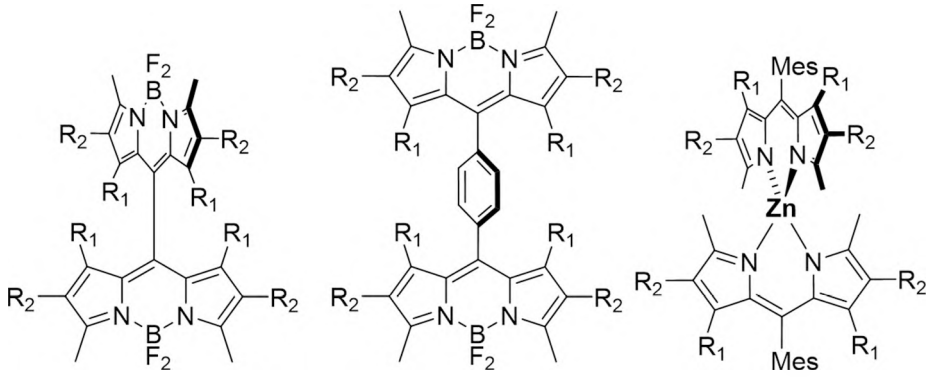

	R_1	R_2
m_4B	H	H
m_8B	Me	H
e_4m_8B	Me	Et

	R_1	R_2
m_4Ph	H	H
m_8Ph	Me	H
e_4m_8Ph	Me	Et

	R_1	R_2
zDIP2	H	H
zDIP3	Me	H

Prior work by our group investigated SBCT within **m_4B** and **m_4Ph**[1]. We found SBCT was significantly faster in **m_4B** than **m_4Ph** and ascribed this to the shorter distance separating **m_4B**'s BODIPY units. However, the lifetime of the SBCT state in **m_4B** was much longer than in **m_4Ph** which is counterintuitive as the shorter distance between **m_4B**'s chromophores should better favor charge recombination. Rather, we attributed the fast charge recombination of **m_4Ph**'s SBCT state to rotation of the phenylene bridge, which can facilitate nonradiative decay. Below, we test this hypothesis by exploring systems where steric constraints limit bridge rotation.

We have also looked at a series of **zDIP**s (**Scheme 1**) where formation of a SBCT state was identified by spectroelectrochemistry and femtosecond-to-millisecond TA[2]. Reported **zDIP**s were discussed in terms of their solvent-dependent excited state properties as a function of substitution on the dippyrinato ligands (**DIP**)[52]. In another study **zDIP2** was used to probe how the free energy difference between the SBCT and LE states (ΔG^0_{SBCT}) changed with solvent dielectric

to identify a local environment that gave no driving force for their interconversion (*i.e.* $\Delta G^0_{SBCT} = 0$ for the LE ⇄ SBCT reaction).[3] This was found for a mixture of 20% tetrahydrofuran (THF) to 80% cyclohexane (CHX) with an $E_T(30) \sim 34$.

Herein, we expand upon this work by comparing the ground-state structure and photoexcited dynamics of six BODIPY dimers, three directly linked through their *meso* positions (**Scheme 1: m_4B, m_8B, e_4m_8B**) and three incorporating a phenylene bridge between the dimers (**Scheme 1: m_4Ph, m_8Ph, e_4m_8Ph).** Due to steric hindrance, the BODIPY units of **m_nB** are held in near orthogonal configurations while the phenylene bridge in **m_nPh** both increases dimer spatial separation and allows the BODIPY dyes to occupy a common plane. We also compare the dynamics of **m_nB** and **m_nPh** to analogous zinc-bridged dipyrrinato dimers (**zDIP2/zDIP3**) that afford a similar spatial separation between dipyrrin chromophores but orient them in a rigid, orthogonal geometry.

Interchromophore Separation

Chromophore spatial separation within a molecular dimer is expected to play a major role in SBCT[21,53]. Electron transfer is promoted by orbital overlap, which has an exponential dependence on donor and acceptor separation[54–56]. Going from **m_nB** to **zDIP** to **m_nPh**, the center to center distance of each dimer increases from 4.5 Å to 6.4 Å to 8.8 Å. To begin, we compare **m_8B**, **zDIP2** and **m_8Ph** to assess the impact of interchromophore spatial separation on SBCT in systems with a similar degree of steric encumbrance.

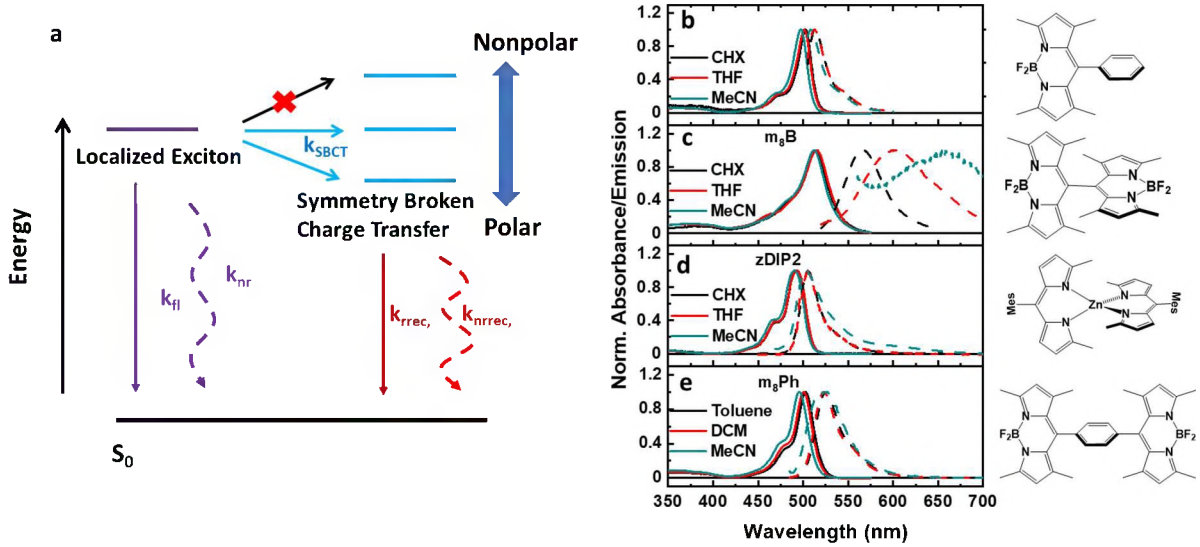

Figure 3: (a) Jablonskii diagram for SBCT showing the impact of solvent polarity. LE states produced by light can undergo SBCT ($\mathbf{k_{SBCT}}$) or return to the ground state via radiative ($\mathbf{k_{fl}}$) and nonradiative ($\mathbf{k_{nr}}$) decay channels. As solvent polarity is increased, the SBCT state is stabilized, making its formation from the LE state exoergic. From the SBCT state, the system can decay radiatively ($\mathbf{k_{rrec}}$) and nonradiatively ($\mathbf{k_{nrrec}}$). (b-e) Absorption and emission spectra of (b) **1,3,5,7-tetramethyl-8-phenyl-BODIPY**, (c) $\mathbf{m_8B}$, (d) **zDIP2,** and (e) $\mathbf{m_8Ph}$. Absorption spectra of all four systems are similar. Emission spectra of $\mathbf{m_8B}$ are solvatochromically-shifted, indicating an emissive SBCT state, while **zDIP2** and $\mathbf{m_8Ph}$ emission is dominated by their LE states.

Steady-state absorption spectra of $\mathbf{m_8B}$**, zDIP2** and $\mathbf{m_8Ph}$ provide insight into interdimer electronic coupling (**Figures 3b-e**). Spectra of $\mathbf{m_8Ph}$ (**Figure 3e**) are similar to the **1,3,5,7-tetramethyl-8-phenyl-BODIPY** monomer (**Figure 3b)**, indicating minimal electronic coupling between $\mathbf{m_8Ph}$'s phenylene-bridged BODIPY chromophores. This behavior can be contrasted with that of $\mathbf{m_8B}$ (**Figure 3c**), which contains identical chromophores but lacks the central phenyl ring of $\mathbf{m_8Ph}$. Absorption spectra of $\mathbf{m_8B}$ are bathochromically shifted with respect to that of $\mathbf{m_8Ph}$, suggesting enhanced interchromophore coupling within $\mathbf{m_8B}$ stemming from the proximity of its BODIPY units. This spectral redshift is seen for all $\mathbf{m_nB}$ dimers (**Figure S1**). Absorption spectra

Table 1: Photophysical Properties of Dipyrrin Dimers.

	Solvent	Absorption λ_{max1} (λ_{max2}) (nm)	Emission λ_{max} (nm)	Stokes Shift (cm^{-1})	Φ_{PL}
1,3,5,7-Me$_4$-8-Phenyl-BODIPY	Cyclohexane THF MeCN	502 501 497	514 512 509	465 429 474	0.56 0.52 0.62
m$_4$B	Toluene DCM MeCN	533 (544) 530 (543) 527 (541)	577 619 --	1,051 2,261	0.62[a] 0.087[a] 0.008
m$_4$Ph	Toluene DCM MeCN	515 513 508	540 538 531	899 905 853	0.095[a] 0.069[a] 0.010
m$_8$B	Cyclohexane THF DCM MeCN	514 515 512 515	566 602 (646) 613 (647) 654	1,787 2,806 3,218 4,127	0.70 0.14 0.14 0.014
m$_8$Ph	Toluene DCM MeCN	503 501 495	520 513 (520) 520	650 729 971	0.52 0.31 0.027
e$_4$m$_8$B	Toluene DCM MeCN	543 541 538	592 634 684	1,524 2,711 3,967	--
e$_4$m$_8$Ph	Toluene DCM MeCN	525 526 520	546 544 538	732 629 643	0.67 0.52 0.017
zDIP2	Cyclohexane THF MeCN	493 493 490	506 507 508	521 560 723	0.66[b] 0.09[b] 0.005
zDIP3	Cyclohexane THF DCM	489 489 488	507 511 509 (653)	726 880 845	0.16[b] 0.15[b] 0.02[b]

[a]Ref. [1].

[b]Ref. [2]

of **zDIP2** exhibit a slight blue shift (~50 meV) relative to the BODIPY monomer, **m$_8$Ph**, and **m$_8$B** (**Figure 3d, Table 1**). While spectra of all three dimers display slight spectral shifts relative to their parent monomer, the absorption profile of each shows a vibronic progression resembling that of the monomer, suggesting the dimers possess an absorptive LE state similar in character to the

excited monomer.

Steady-state emission spectra were recorded to assess charge transfer in these systems (**Figure 3b**, right). Population transfer from the LE state to an emissive, low-energy state will yield a large emission Stokes shift relative to the parent monomer. If this emissive state carries significant SBCT character, placing the dimer in a polar solvent will further redshift the emission (**Figure 3a,** $\mathbf{k_{rrec}}$) and broaden its linewidth relative to that of the monomer[21,22]. This behavior is observed for **m8B** (**Figure 3c**), whose emission spectra show a progressive bathochromic shift with increasing solvent polarity, signaling formation of an emissive SBCT state.

If SBCT instead results in charges that are decoupled from one another, recombination will likely proceed nonradiatively[21] (**Figure 3a,** $\mathbf{k_{nrrec}}$), yielding a decrease in dimer photoluminescence quantum yield ($\mathbf{\Phi_{PL}}$) with increasing stability of the SBCT state. **zDIP2** and **m8Ph** display emission spectra that are near mirror images of the LE state absorption with a small Stokes shift, suggesting emission originates from the LE state itself (**Figure 3a**, $\mathbf{k_{fl} + k_{nr}}$). This LE emission $\mathbf{\Phi_{PL}}$ decreases with increasing solvent polarity, indicating competition between LE emission and SBCT.

By increasing the BODIPY separation, the coupling between the radical pair produced by SBCT weakens. This can allow population of other states, such as triplet levels, in addition to nonradiative charge recombination (**Figure 3a,** $\mathbf{k_{nrrec}}$). Weak coupling among separated charges in the zinc- and phenyl-bridged systems could allow radical-pair or spin-orbit ISC to a triplet state while more strongly coupled systems may favor charge recombination to the ground state[27]. Distinction of such scenarios requires tracking the excited state dynamics of each dimer, which is most readily achieved with femtosecond TA.

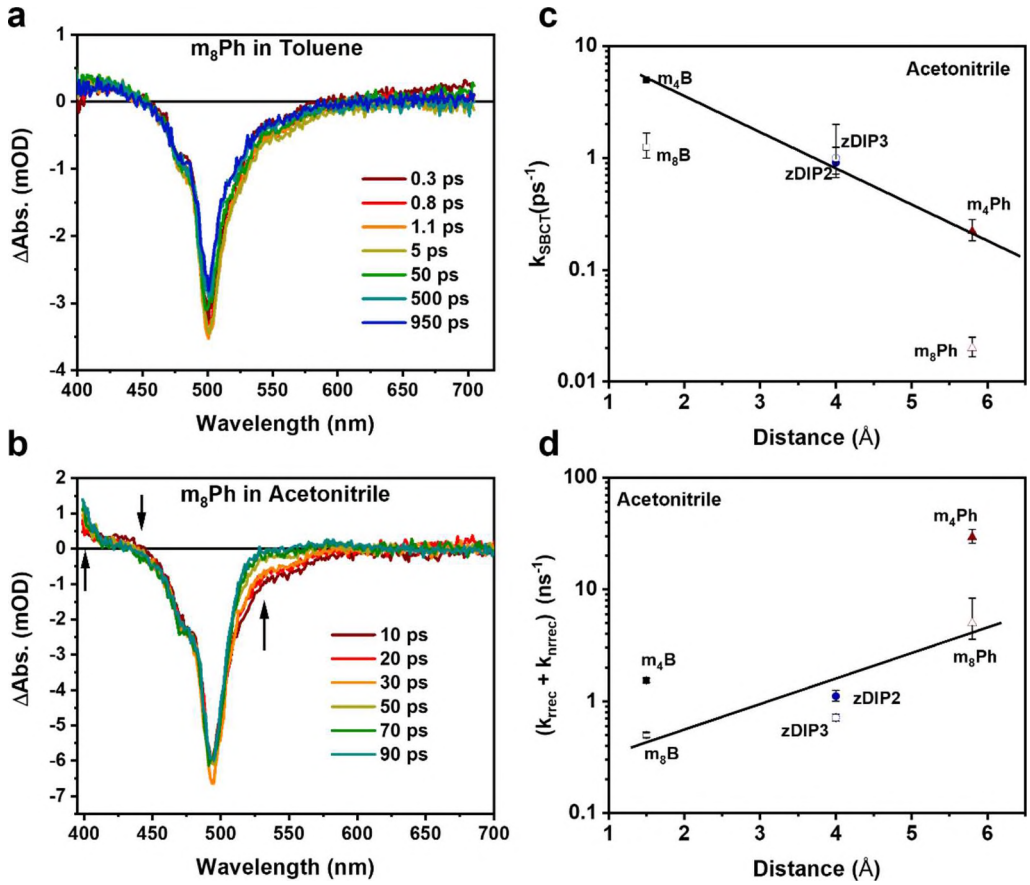

Figure 4. (a) TA spectra of **m8Ph** in toluene where SBCT is not observed, giving only the LE state transient spectrum. (b) TA spectra of **m8Ph** in acetonitrile, where **m8Ph** shows growth of a new ESA feature indicating SBCT. (c) The SBCT rate, k_{SBCT}, versus interchromophore separation in acetonitrile. The solid line shows the expected exponential decrease in this rate with increasing interchromophore separation. (d) Decay rate of the SBCT state, k_{rec}, ($k_{rec} = k_{rrec} + k_{nrrec}$,, **Fig. 2a)** primarily by charge recombination, as a function of interchromophore separation. The solid line is a guide to the eye. In c and d, squares, circles and triangles denote the directly linked, zinc-bridged and phenylene-bridged dimers, respectively. Filled shapes represent dimers with methyl substituents on the 1 and 7 position of the BODIPY core, while open symbols correspond to dimers with methyl substituents at the 1, 3, 5 and 7 positions of the BODIPY core. This shows an unexpected result as closely spaced dimers undergo charge recombination more slowly than further spaced dimers.

Figures 4a and **4b** plot TA spectra of **m8Ph** in toluene and acetonitrile (MeCN), respectively, following excitation at 500 nm. At short time delays, a strong negative signal is seen at 490 nm that corresponds to the dimer's ground state bleach (GSB) and signifies formation of excited molecules. An additional negative shoulder at ~525 nm denotes stimulated emission (SE) that indicates these molecules are in the LE state. In toluene, the TA spectra remain invariant as a

function of time. In MeCN, however, the SE feature disappears while the GSB is unchanged. The disappearance is associated with a rise in a new excited state absorption (ESA) superimposed with the SE, signaling a transition from the LE state to a new excited state we have previously identified as the SBCT state[1,19].

Figures 4c and **4d** summarize rates for formation and decay of the SBCT state, $\mathbf{k_{SBCT}}$ and $\mathbf{k_{rec}}$ ($\mathbf{k_{rec}} = \mathbf{k_{rrec}} + \mathbf{k_{nrrec}}$), extracted from TA data recorded in MeCN for several dyads with differing interchromophore separation (**Table 2**). Though the rates of SBCT and recombination will depend on the change in free energy between the LE and SBCT states (ΔG^0_{SBCT}), and SBCT and ground states (ΔG^0_{CR}), respectively, it can be seen in **Table S1** (**Supporting Information**) that the effect of substitution changes are modest (the respective driving force varies only by ~100 meV for a single solvent). Changing the chromophore separation of the BODIPY chromophores also changes the energy of the SBCT state because of the decreasing Coulomb stabilization between the anion and cation portions of the charge separated state. Calculations suggest that the driving force is consequently reapportioned between the two charge transfer processes but again only by ~100 meV.

In polar MeCN, the SBCT state is highly stabilized and TA spectra are best fitted by a model that postulates population transfer from the LE state to SBCT state (LE □ SBCT) followed by decay of the SBCT state to either the ground or, in the case of **zDIP**s, additionally to a triplet state[2]. For less polar solvents, backward electron transfer to return the system to the LE state, $\mathbf{k_{BET}}$, also needs to be considered. It is relevant only for the smaller values of ΔG^0_{SBCT} (<200 meV, and fully described in Kellogg et. al[3] in the context of zDIP2); it is included in the model when an equilibrium between LE and SBCT state is required to achieve a good fit the spectral data.

As expected, $\mathbf{k_{SBCT}}$ decreases with increasing interchromophore spatial separation (**Figure**

4c) which is accompanied by smaller driving force (Table S1). $\mathbf{k_{SBCT}}$ for **m4B**, **zDIP2**, and **m4Ph** exhibit an exponential dependence on interchromophore separation, while **m8B, zDIP3** and **m8Ph** do not follow a single exponential decay which may relate to an observed intermediate PCT state (see detail in the **SI**). Moving to less polar solvents, $\mathbf{k_{SBCT}}$ slows for each dyad (**Table 2**) as nonpolar solvents are less able to reorganize to stabilize the SBCT state. However, for a given solvent, the overall trend of $\mathbf{k_{SBCT}}$ (decreasing as interchromophore separation increases while driving force is simultaneously reduced) is maintained (see **SI** for TA spectra)*;* SBCT is dependent on orbital overlap and driving force, and thus both are disfavored by increasing dimer separation.

We would also expect the **mnB** dimers to show the fastest $\mathbf{k_{rec}}$ among our dimer series as the resulting electron and hole are held in the closest proximity to one another, aiding their recombination. Energetics in this case should work in the same direction: the steady-state absorption and emission spectra (**Table 1**) show the **mnB** dimers have their LE state closer to the ground state relative to **mnPh** dimers; furthermore, the calculated ΔG^0_{SBCT} (**Table S1**) show SBCT states lie lower still for the **mnB** dimers than the **mnPh** dimers. Taken together, ΔG^0_{CR} is *smallest* for the **mnB** dimers and so a faster $\mathbf{k_{nrrec}}$ would be expected by the energy gap law (if energetics alone were considered). However, in all solvents increasing interchromophore separation showed behavior *opposite* to expectations. As interchromophore separation is increased, $\mathbf{k_{nrrec}}$ increases (the lifetime of the SBCT state decreases). In polar MeCN for example, this effect is significant as the **m8B** SBCT state exhibits a 2 ns lifetime that is about 2× longer than **zDIP2** (0.9 ns) and 9× longer than that of **m8Ph** (0.2 ns).

Table 2: Kinetic rates for transitions between excited states of dipyrrin dimers determined by femtosecond TA, time-resolved and steady state fluorescence.

	Solvent	$1/k_{SBCT}$ ($1/k_{BET}$) (ps)	$1/(k_{rrec}+k_{nrrec})$[a] (ps)	$1/(k_{fl}+k_{nr})$[a] (ps)
m_4B	Toluene	6.5±2		--
	DCM	1±1	7000±14	
	Acetonitrile	< 0.2	650±30[b]	
m_8B	Cyclohexane	--	9900±200*	--
	Toluene	7±1	12100±200	
	THF	1.4±0.2	9780±20	
	Acetonitrile	0.8±0.2	2000±100	
e_4m_8B	Toluene	--	9400±500*	--
	DCM	1.3±0.1	9400±500	
	Acetonitrile	0.8±0.3	1700±90	
m_4Ph	Toluene	--	--	845[1]
	DCM	18±5	--	1000[1]
	Acetonitrile	4.5±1	34±5[b]	
m_8Ph	Toluene	--	--	4700±90
	DCM	130±20 (140±20)	--	5170±10
	Acetonitrile	50±10	200±80[b]	
e_4m_8Ph	Toluene	--	--	6810±60
	DCM	140±40 (240±80)	--	7240±140
	Acetonitrile	75±10	280±30[b]	
zDIP2	Cyclohexane[2]	--	--	4800±300
	Toluene[2]	9±2 (16±2)	4000±500	3900±300
	THF[3]	2±0.2 (27±7)	2200±140	4400±20
	Acetonitrile[2]	1.1±0.3	900±100	
zDIP3	Cyclohexane[2]	--	--	1400±300
	Toluene[2]	2.3±1 (11.2±3)	2500±300	2100±200
	Acetonitrile[2]	1.0±0.5	1400±100	

Reference citations to previously published data are given.

* This inverse rate refers to decay of the PCT state; a full SBCT state is not observed in cyclohexane.

[a] Decay rates from the SBCT and LE states were measured using time-resolved fluorescence.

[b] Determined using Transient Absorption

Clearly, interchromophore spatial separation alone is not a sufficient predictor for the decay rate of the SBCT state. The zinc-bridged dipyrrin systems are a classic case of an SBCS system,

where the resulting charges are fully decoupled as the zinc acts as an electronically non-interacting spacer that prevents any through-bond linkage of the dipyrrins. The **zDIP** systems show population of a triplet state following SBCT[2,27], which is encompassed in $\mathbf{k_{nrrec}}$, whereas **m8Ph** and **m8B** decay directly to the ground state. Decay to a triplet state close in energy to the SBCT state may rationalize why **zDIP2** exhibits a faster than expected value for $\mathbf{k_{rec}}$ but does not explain the fast decay rate of **m8Ph** relative to the directly linked **mnB** dimers.

A key difference is recombination is required to take place from a more or less orthogonal geometry (minimum in the SBCT state surface, **Figure 2**) whereas spatial overlap can be modulated for the initial SBCT process by motion on the LE surface. The orthogonal dimer orientation for both **mnB** and **zDIP** systems can reduce the potential for achieving such overlap, thereby slowing the rate of charge recombination relative to **mnPh,** whereas the BODIPY building blocks are closer to a more coplanar arrangement. We test this hypothesis below by modifying the structure of these dimers with steric groups that impact their ability to twist about their meso linkage.

Structural Rigidity and Chromophore Configuration

We have identified a decrease in the SBCT state lifetime with increasing chromophore separation that runs counter to expectation (**Figure 4d**). Here, we discuss the role of molecular conformation on interchromophore wavefunction overlap, which modulates the rate of decay from the SBCT state ($\mathbf{k_{rec}}$). Examining **Figure 1c**, we see that within a minimal 4-electron model both $\mathbf{k_{SBCT}}$ and $\mathbf{k_{nrrec}}$ are expected to be dependent on the spatial overlap of the frontier orbitals of the dimer but exhibit different dependencies on the overlaps between pairs of orbitals. While $\mathbf{k_{SBCT}}$ is dependent on both the LUMO-LUMO and HOMO-HOMO overlap of the pair, $\mathbf{k_{nrrec}}$ instead depends on the dimer's HOMO-LUMO overlap. Due to the different symmetries of these orbitals,

this suggests that geometries may be found that maximize $\mathbf{k_{SBCT}}$ while suppressing $\mathbf{k_{nrrec}}$.

To identify structures enhancing $\mathbf{k_{SBCT}}$ over $\mathbf{k_{nrrec}}$, we used DFT to compute the frontier orbitals of $\mathbf{m_4B}$ as a function of its torsion angle. A diabatization procedure was used to project these orbitals onto linear combinations of the HOMO and LUMO orbitals of the BODIPY monomer to deduce how coupling between the HOMO and LUMO orbitals of the $\mathbf{m_4B}$ dimer change with torsion angle (**Figure 5**). Note that we find the HOMO and LUMO of the BODIPY monomer to be very similar to SOMOs of its radical cation and anion states, indicating that we can use coupling between the HOMO and LUMO to examine the impact of torsion on both SBCT and charge recombination.

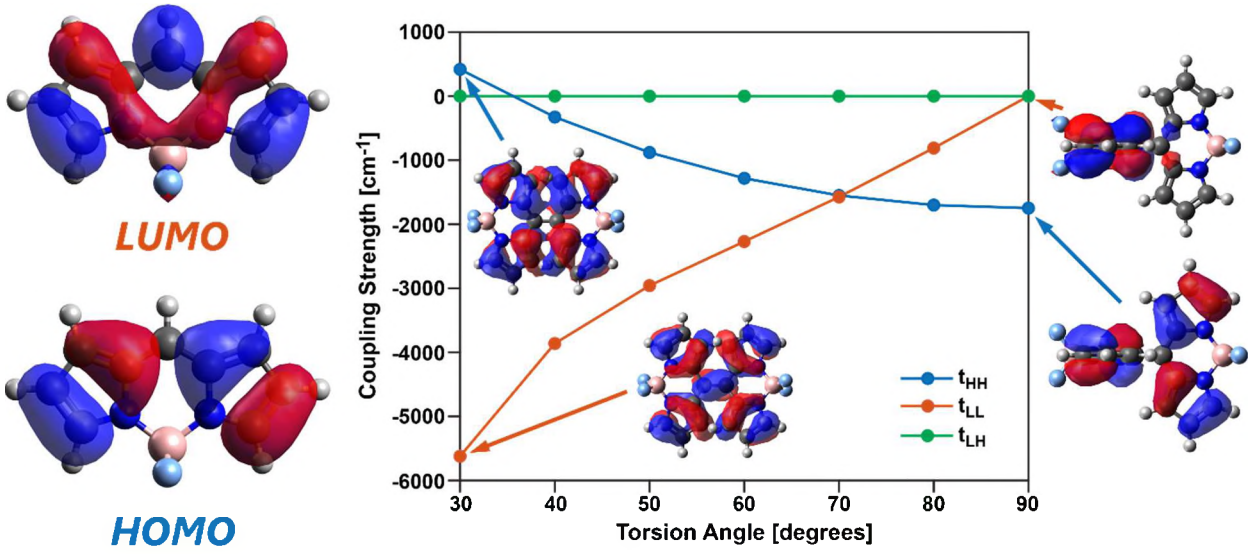

Figure 5: (Left) DFT calculations of the HOMO and LUMO of the ground state BODIPY dyads using cam-B3LYP. (Right) Coupling strength as a function of torsional angle. Though both the HOMO-HOMO and LUMO-LUMO coupling depend on the torsional angle, the HOMO-LUMO coupling is zero for all angles. The distance between the two dyads is fixed at 1.4 Å, so the above illustration should be taken as qualitative as the electronic coupling will be distance dependent.

We find that the LUMO-LUMO coupling is minimal when $\mathbf{m_4B}$'s dihedral angle is 90° while coupling between the HOMO orbitals of the BODIPY fragments is maximized at this angle. This suggests SBCT involving the transfer of an electron across the bridge from the excited

fragment in a rigidly held dimer is suppressed while hole transfer may be possible. Interestingly, we find that as the torsion angle decreases, the HOMO-HOMO coupling decreases while the LUMO-LUMO coupling increases. Notably however, the LUMO-LUMO coupling increase outpaces the HOMO-HOMO coupling decrease, suggesting that relaxation of the dimer torsional rigidity should enhance the rate of SBCT. This is supported by observations for bis-DIPYR and bis-α-DIPYR systems[50] where the systems of interest were dispersed into a polymer matrix with a similar dielectric to toluene and THF, respectively. With the matrix impeding torsion of the dimers, SBCT was very slow.

Examining the HOMO-LUMO coupling, we find that the opposite symmetry of the HOMO and LUMO orbitals ensures that this coupling is zero regardless of **m4B**'s torsion angle. This implies that unlike SBCT, torsion-induced variation in the rate of charge recombination does not stem from changes in orbital overlap of the BODIPY fragment units. Rather, the dominant mechanism by which torsion impacts nonradiative decay is by bringing the ground state into energetic resonance with the SBCT state (**Figure 2, Figure S1**). At such a point, other internal vibrational degrees of freedom can act to nonadiabatically couple these two states, leading to the return of population to the ground state. Vibrational degrees of freedom of SBCT have been studied using time resolved infrared spectroscopy[15,47,57]; this probe was used to examine how structural fluctuations give different pathways to SBCT and subsequent recombination. The addition of steric groups that hinder rotation along the meso linkage will stiffen the SBCT potential and reduce the ability of the dimer to access geometries where return to the ground state is possible, thereby slowing $\mathbf{k_{nrrec}}$.

To experimentally test these hypotheses regarding the impact of interdimer rotation on $\mathbf{k_{SBCT}}$ and $\mathbf{k_{nrrec}}$, we increased the steric rigidity of meso-bridged BODIPY dimers by substituting

methyl groups that hinder dihedral rotation about the C – C bond tethering directly linked dimers (**m_8B**, **e_4m_8B**) and rotation about the bridge of phenylene-linked systems (**m_8Ph**, **e_4m_8Ph**). The structural rigidity of the directly linked dimers is apparent in their steady-state spectra. **m_4B**'s absorption spectra (**Figure S1**) have a primary absorption peak (λ_{max1}, **Table 1**) with a weaker red shoulder (λ_{max2}, **Table 1**) resembling the spectral pattern of an H-aggregate. This reflects excitonic splitting from coupling of the BODIPY transition moments, signaling that its chromophores are not orthogonal. This contrasts with **m_8B** and **e_4m_8B**, where only a single transition appears in their absorption spectra, which is to be expected if the two transition dipoles are rigorously orthogonal to each other.

With increasing steric hindrance about the meso bridge, directly linked dimers show a decrease in their SBCT rate (**Figure 6**). The reduced rate of SBCT in the more rigid BODIPY dimers implies surface crossing to the SBCT state is disfavored as the LUMO-LUMO overlap is greatly reduced. Though the HOMO-HOMO overlap increases, the relative HOMO-HOMO coupling strength is significantly less than LUMO-LUMO overlap for the less sterically constrained compounds, resulting in a k_{SBCT} nearly an order of magnitude slower in **m_8B** and **e_4m_8B** (0.8 ps, MeCN) relative to **m_4B** (0.1 ps, MeCN). While k_{SBCT} is slower in the rigid, directly linked dyads, the lifetime of their SBCT state is also longer (**Figure 6**). In MeCN, k_{rec} is almost three times slower in **m_8B** (2 ns) and **e_4m_8B** (1.7 ns) than **m_4B** (0.65 ns). These observations are consistent with our hypothesis that systems with higher torsional rigidity will exhibit longer SBCT state lifetimes because of a higher barrier to reaching resonance between the ground and SBCT surfaces.

With the **m_nPh** dimers, increasing steric crowding diminishes the ease of bridge rotation and thus through bond coupling between pendant BODIPY chromophores. In **Figure 6** we see

that for **m8Ph** this both reduces k_{SBCT} and increases the longevity of the SBCT state. In MeCN, the time constants for SBCT in **m4Ph** and **m8Ph** differ by an order of magnitude, 4.5 ps and 50 ps, respectively. By fixing the phenylene bridge to be orthogonal to the BODIPY planes, k_{SBCT} is slowed as the through-bond HOMO-HOMO and LUMO-LUMO interaction is decreased. As with the directly linked dimers, the lifetime of the SBCT state also increases (slower k_{rec}) with decreasing torsional freedom, from 34 ps to 200 ps moving from **m4Ph** to **m8Ph**.[37,46] While we are able to reduce k_{rec} for the phenylene-bridged dimers, they still exhibit the shortest SBCT lifetimes by about an order of magnitude relative to the directly linked and zinc-bridged dimers. This may stem from vibrational modes along the phenylene bridge which further de-symmetrizes the excited system, mediating charge transfer.

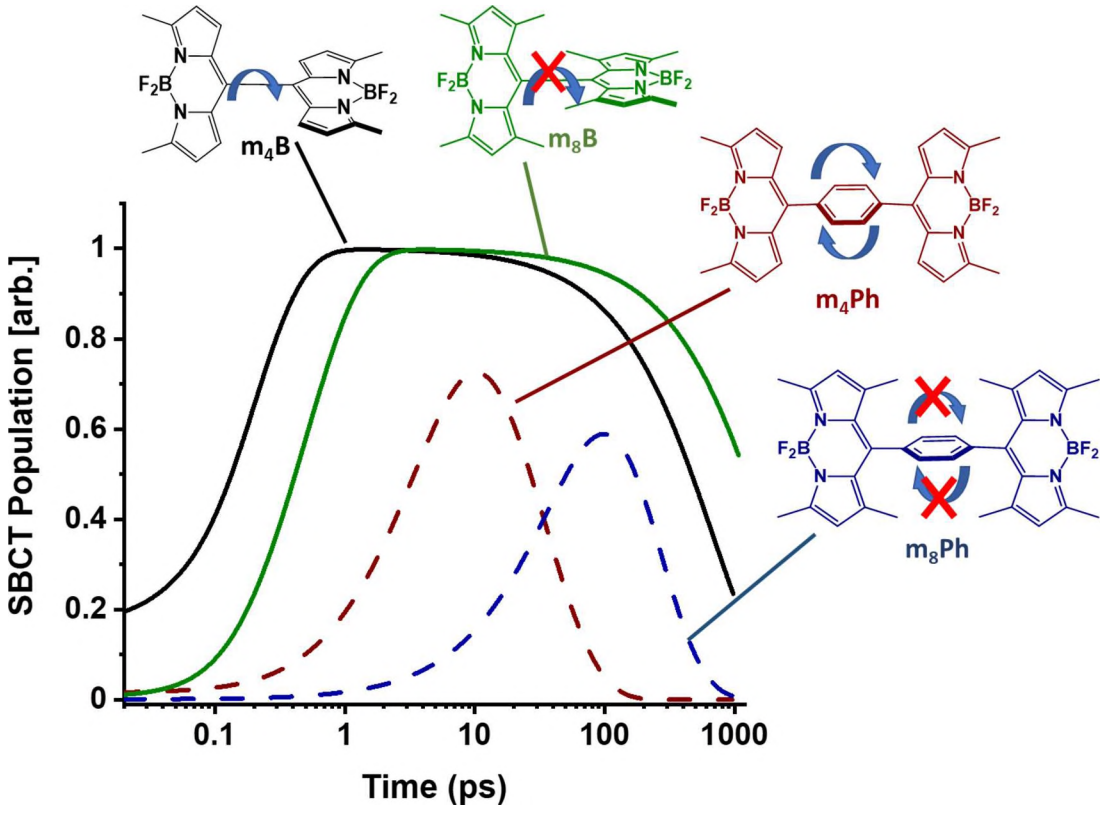

Figure 6: SBCT state population as a function of time for **m4B** (black solid line), **m8B** (green solid line), **m4Ph** (red dashed line) and **m8Ph** (blue dashed line) taken from global analysis fits of SBCT in MeCN (see Supporting Information).

Our results indicate that the rate of SBCT and longevity of the resultant charge-separated state can be tuned independently. This is shown in **Figure 4** and **6**, where the rate of SBCT scales with interchromophore spatial separation but is modified by the torsional rigidity of the dimer.

Summary & Outlook

The excited state and electrochemical properties of dipyrrins make them advantageous platforms for organic photovoltaic and solar fuel generation via artificial photosynthesis. We have found SBCT efficiency to be dependent on several intramolecular properties, including interdimer spatial separation as well as chromophore electronic coupling introduced by variations in chemical bonding and molecular structure. The SBCT state lifetime is not simply dependent on interdimer separation but requires careful analysis of vibronic coupling to non-totally symmetric vibrational modes to induce coupling. Importantly, a rigidly orthogonal dimer, even at close proximity, can give rise to long-lived SBCT states. We have observed orthogonal BODIPY dimers showing a figure of merit of k_{CR}/k_{SBCT} between 1,400 - 4,000 in acetonitrile, similar to recently reported for similarly configured PDI-dimers.[18] In some cases we observe an intermediate PCT state for directly linked systems; this is well known for the BA system and fully discussed in the **SI** and may impact SBCT formation. These design principles can be used to design new molecular systems that rapidly form long-lived, spatially separated charges upon photoexcitation.

Supporting Information Available

Description of experimental and theoretical methods, global target analysis, calculation for ΔG^0_{SBCT} and ΔG^0_{CR}, and calculations for orbital overlap and ground state potential energy surfaces (PES) as a function of dihedral angle of the BODIPY dyads and separate *.xyz files used for these orbital overlap and ground state PES calculations. Steady-state absorption, emission and transient

absorption spectra of BODIPY dimers and their fits using global target analysis. Discussion of an observed PCT state in transient measurements.

Acknowledgements

This research is supported by the United States Department of Energy, Office of Basic Energy Sciences, Solar Photochemistry program under DE-SC0016450. L.E. was also supported by a Norma and Jerol Sonosky Summer Fellowship at USC. STR thanks support from the Welch Foundation (Grant F-1885) and the Alfred P. Sloan Foundation via a Research Fellowship. NVK and JM acknowledge support from the Department of Energy, Office of Basic Energy Sciences, Division of Chemical Sciences, Biosciences, and Geosciences, under award number DE-SC0007004. Work by D.E.C. was supported the National Science Foundation under grant CHE-1654404. The authors also acknowledge the Texas Advanced Computing Center (TACC) at The University of Texas at Austin for providing computing resources.

Biographical Information

Laura Estergreen earned her Ph.D. at the University of Southern California (USC) working with Stephen Bradforth and is currently a Postdoctoral Researcher with Sean Roberts at the University of Texas at Austin (UTA) where she builds instrumentation for high temporal and spatial resolution microscopy.

Austin Menke is a Ph.D. candidate with Mark Thompson at USC. His research focuses on materials for organic electronics.

Daniel Cotton is a Ph.D. candidate with Sean Roberts at UTA. His research focuses on how intermolecular coupling dictate the electronic properties of molecular solids and correlating these with even-order nonlinear spectroscopies.

Nadezhda Korovina is an Assistant Professor of Chemistry and Biochemistry at California State University, Chico. Her research focuses on understanding photophysical processes of organic compounds for optoelectronic devices.

Josef Michl is Professor of Chemistry at the University of Colorado, Boulder, and a Member of the National Academy of Sciences. His research deals with theoretical and experimental aspects of organic photochemistry and photophysics, preparation of organic and inorganic reactive intermediates, theory of sigma electron delocalization, and 2-D polymers.

Sean Roberts is an Associate Professor and a Fellow of the William H. Wade Endowed Professorship in Chemistry at UTA. His group employs ultrafast spectroscopy to understand how molecular materials manipulate energy, charge, and spin.

Mark Thompson is the Ray R. Irani Chair of Chemistry at the USC and a member of the National Academy of Engineering. His research interests include materials for organic electronics, principally organic LEDs and solar cells.

Stephen Bradforth is a Professor of Chemistry at USC. His lab designs experiments to probe how interconnected molecular motions guide chemical reactions in complex environments, such as in liquids or in functional molecular materials.

References

(1) Whited, M. T.; Patel, N. M.; Roberts, S. T.; Allen, K.; Djurovich, P. I.; Bradforth, S. E.; Thompson, M. E. Symmetry-Breaking Intramolecular Charge Transfer in the Excited State of Meso -Linked BODIPY Dyads. *Chem Commun* **2011**, *48* (2), 284–286. https://doi.org/10.1039/c1cc12260f.

(2) Trinh, C.; Kirlikovali, K.; Das, S.; Ener, M. E.; Gray, H. B.; Djurovich, P.; Bradforth, S. E.; Thompson, M. E. Symmetry-Breaking Charge Transfer of Visible Light Absorbing Systems: Zinc Dipyrrins. *J Phys Chem C* **2014**, *118* (38), 21834–21845. https://doi.org/10.1021/jp506855t.

(3) Kellogg, M.; Akil, A.; Ravinson, D. S. M.; Estergreen, L.; Bradforth, S. E.; Thompson, M. E. Symmetry Breaking Charge Transfer as a Means to Study Electron Transfer with No Driving Force. *Faraday Discuss* **2019**, *216* (0), 379–394. https://doi.org/10.1039/c8fd00201k.

(4) Brinkert, K. Energy Conversion in Natural and Artificial Photosynthesis. **2018**. https://doi.org/10.1007/978-3-319-77980-5.

(5) Grondelle, R. van; Dekker, J. P.; Gillbro, T.; Sundstrom, V. Energy Transfer and Trapping in Photosynthesis. *Biochimica Et Biophysica Acta Bba - Bioenergetics* **1994**, *1187* (1), 1–65. https://doi.org/10.1016/0005-2728(94)90166-x.

(6) Suga, M.; Akita, F.; Hirata, K.; Ueno, G.; Murakami, H.; Nakajima, Y.; Shimizu, T.; Yamashita, K.; Yamamoto, M.; Ago, H.; Shen, J.-R. Native Structure of Photosystem II at 1.95 Å Resolution Viewed by Femtosecond X-Ray Pulses. *Nature* **2015**, *517* (7532), 99–103. https://doi.org/10.1038/nature13991.

(7) El-Kabbani, O.; Chang, C. H.; Tiede, D.; Norris, J.; Schiffer, M. Comparison of Reaction Centers from Rhodobacter Sphaeroides and Rhodopseudomonas Viridis: Overall Architecture and Protein-Pigment Interactions. *Biochemistry-us* **1991**, *30* (22), 5361–5369. https://doi.org/10.1021/bi00236a006.

(8) Deisenhofer, J.; Epp, O.; Miki, K.; Huber, R.; Michel, H. X-Ray Structure Analysis of a Membrane Protein Complex Electron Density Map at 3 Å Resolution and a Model of the Chromophores of the Photosynthetic Reaction Center from Rhodopseudomonas Viridis. *J Mol Biol* **1984**, *180* (2), 385–398. https://doi.org/10.1016/s0022-2836(84)80011-x.

(9) Chang, C.-H.; Tiede, D.; Tang, J.; Smith, U.; Norris, J.; Schiffer, M. Structure of Rhodopseudomonas Sphaeroides R-26 Reaction Center. *Febs Lett* **1986**, *205* (1), 82–86. https://doi.org/10.1016/0014-5793(86)80870-5.

(10) *Reaction Centers of Phtosynthetic Bacteria*, 1st ed.; Mchel-Beyerle, M.-E., Ed.; Springer Series in Biophysics; Springer-Verlag Berlin Heidelberg, 1990; Vol. 6. https://doi.org/10.1007/978-3-642-61297-8_43.

(11) Breton, J.; Martin, J.-L.; Migus, A.; Antonetti, A.; Orszag, A. Femtosecond Spectroscopy of Excitation Energy Transfer and Initial Charge Separation in the Reaction Center of the Photosynthetic Bacterium Rhodopseudomonas Viridis. *Proc National Acad Sci* **1986**, *83* (14), 5121–5125. https://doi.org/10.1073/pnas.83.14.5121.

(12) Wasielewski, M. R. Photoinduced Electron Transfer in Supramolecular Systems for Artificial Photosynthesis. *Chem Rev* **1992**, *92* (3), 435–461. https://doi.org/10.1021/cr00011a005.

(13) Deisenhofer, J.; Norris, J. R. *Photosynthetic Reaction Center* ; Academic Press: San Diego, 1993; Vol. 2. https://doi.org/https://doi.org/10.1016/C2009-0-02601-4.

(14) Veldkamp, B. S.; Han, W.-S.; Dyar, S. M.; Eaton, S. W.; Ratner, M. A.; Wasielewski, M. R. Photoinitiated Multi-Step Charge Separation and Ultrafast Charge Transfer Induced Dissociation in a Pyridyl -Linked Photosensitizer–Cobaloxime Assembly. *Energ Environ Sci* **2013**, *6* (6), 1917–1928. https://doi.org/10.1039/c3ee40378e.
(15) Kim, T.; Kim, W.; Mori, H.; Osuka, A.; Kim, D. Solvent and Structural Fluctuations Induced Symmetry-Breaking Charge Transfer in a Porphyrin Triad. *J Phys Chem C* **2018**, *122* (34), 19409–19415. https://doi.org/10.1021/acs.jpcc.8b05363.
(16) Yushchenko, O.; Villamaina, D.; Sakai, N.; Matile, S.; Vauthey, E. Comparison of Charge-Transfer Dynamics of Naphthalenediimide Triads in Solution and π-Stack Architectures on Solid Surfaces. *J Phys Chem C* **2015**, *119* (27), 14999–15008. https://doi.org/10.1021/acs.jpcc.5b04060.
(17) Giaimo, J. M.; Gusev, A. V.; Wasielewski, M. R. Excited-State Symmetry Breaking in Cofacial and Linear Dimers of a Green Perylenediimide Chlorophyll Analogue Leading to Ultrafast Charge Separation. *J Am Chem Soc* **2002**, *124* (29), 8530–8531. https://doi.org/10.1021/ja026422l.
(18) Sebastian, E.; Hariharan, M. Null Exciton-Coupled Chromophoric Dimer Exhibits Symmetry-Breaking Charge Separation. *J Am Chem Soc* **2021**, *143* (34), 13769–13781. https://doi.org/10.1021/jacs.1c05793.
(19) Hattori, S.; Ohkubo, K.; Urano, Y.; Sunahara, H.; Nagano, T.; Wada, Y.; Tkachenko, N. V.; Lemmetyinen, H.; Fukuzumi, S. Charge Separation in a Nonfluorescent Donor−Acceptor Dyad Derived from Boron Dipyrromethene Dye, Leading to Photocurrent Generation. *J Phys Chem B* **2005**, *109* (32), 15368–15375. https://doi.org/10.1021/jp050952x.
(20) Hu, R.; Lager, E.; Aguilar-Aguilar, A.; Liu, J.; Lam, J. W. Y.; Sung, H. H. Y.; Williams, I. D.; Zhong, Y.; Wong, K. S.; Peña-Cabrera, E.; Tang, B. Z. Twisted Intramolecular Charge Transfer and Aggregation-Induced Emission of BODIPY Derivatives. *J Phys Chem C* **2009**, *113* (36), 15845–15853. https://doi.org/10.1021/jp902962h.
(21) Kumpulainen, T.; Lang, B.; Rosspeintner, A.; Vauthey, E. Ultrafast Elementary Photochemical Processes of Organic Molecules in Liquid Solution. *Chem Rev* **2016**, *117* (16), 10826–10939. https://doi.org/10.1021/acs.chemrev.6b00491.
(22) Grabowski, Z. R.; Rotkiewicz, K.; Rettig, W. Structural Changes Accompanying Intramolecular Electron Transfer: Focus on Twisted Intramolecular Charge-Transfer States and Structures. *Chem Rev* **2003**, *103* (10), 3899–4032. https://doi.org/10.1021/cr940745l.
(23) Dereka, B.; Svechkarev, D.; Rosspeintner, A.; Tromayer, M.; Liska, R.; Mohs, A. M.; Vauthey, E. Direct Observation of a Photochemical Alkyne–Allene Reaction and of a Twisted and Rehybridized Intramolecular Charge-Transfer State in a Donor–Acceptor Dyad. *J Am Chem Soc* **2017**, *139* (46), 16885–16893. https://doi.org/10.1021/jacs.7b09591.
(24) Fakis, M.; Beckwith, J. S.; Seintis, K.; Martinou, E.; Nançoz, C.; Karakostas, N.; Petsalakis, I.; Pistolis, G.; Vauthey, E. Energy Transfer and Charge Separation Dynamics in Photoexcited Pyrene–Bodipy Molecular Dyads. *Phys Chem Chem Phys* **2017**, *20* (2), 837–849. https://doi.org/10.1039/c7cp06914f.
(25) Kamkaew, A.; Lim, S. H.; Lee, H. B.; Kiew, L. V.; Chung, L. Y.; Burgess, K. BODIPY Dyes in Photodynamic Therapy. *Chem Soc Rev* **2012**, *42* (1), 77–88. https://doi.org/10.1039/c2cs35216h.

(26) Filatov, M. A. Heavy-Atom-Free BODIPY Photosensitizers with Intersystem Crossing Mediated by Intramolecular Photoinduced Electron Transfer. *Org Biomol Chem* **2019**, *18* (1), 10–27. https://doi.org/10.1039/c9ob02170a.
(27) Das, S.; Thornbury, W. G.; Bartynski, A. N.; Thompson, M. E.; Bradforth, S. E. Manipulating Triplet Yield through Control of Symmetry-Breaking Charge Transfer. *J Phys Chem Lett* **2018**, *9* (12), 3264–3270. https://doi.org/10.1021/acs.jpclett.8b01237.
(28) Vauthey, E. Photoinduced Symmetry-Breaking Charge Separation. *Chemphyschem* **2012**, *13* (8), 2001–2011. https://doi.org/10.1002/cphc.201200106.
(29) Margulies, E. A.; Miller, C. E.; Wu, Y.; Ma, L.; Schatz, G. C.; Young, R. M.; Wasielewski, M. R. Enabling Singlet Fission by Controlling Intramolecular Charge Transfer in π-Stacked Covalent Terrylenediimide Dimers. *Nat Chem* **2016**, *8* (12), 1120–1125. https://doi.org/10.1038/nchem.2589.
(30) Sanders, S. N.; Kumarasamy, E.; Pun, A. B.; Trinh, M. T.; Choi, B.; Xia, J.; Taffet, E. J.; Low, J. Z.; Miller, J. R.; Roy, X.; Zhu, X.-Y.; Steigerwald, M. L.; Sfeir, M. Y.; Campos, L. M. Quantitative Intramolecular Singlet Fission in Bipentacenes. *J Am Chem Soc* **2015**, *137* (28), 8965–8972. https://doi.org/10.1021/jacs.5b04986.
(31) Zirzlmeier, J.; Lehnherr, D.; Coto, P. B.; Chernick, E. T.; Casillas, R.; Basel, B. S.; Thoss, M.; Tykwinski, R. R.; Guldi, D. M. Singlet Fission in Pentacene Dimers. *Proc National Acad Sci* **2015**, *112* (17), 5325–5330. https://doi.org/10.1073/pnas.1422436112.
(32) Korovina, N. V.; Das, S.; Nett, Z.; Feng, X.; Joy, J.; Haiges, R.; Krylov, A. I.; Bradforth, S. E.; Thompson, M. E. Singlet Fission in a Covalently Linked Cofacial Alkynyltetracene Dimer. *J Am Chem Soc* **2016**, *138* (2), 617–627. https://doi.org/10.1021/jacs.5b10550.
(33) Johnson, J. C.; Akdag, A.; Zamadar, M.; Chen, X.; Schwerin, A. F.; Paci, I.; Smith, M. B.; Havlas, Z.; Miller, J. R.; Ratner, M. A.; Nozik, A. J.; Michl, J. Toward Designed Singlet Fission: Solution Photophysics of Two Indirectly Coupled Covalent Dimers of 1,3-Diphenylisobenzofuran. *J Phys Chem B* **2013**, *117* (16), 4680–4695. https://doi.org/10.1021/jp310979q.
(34) Alvertis, A. M.; Lukman, S.; Hele, T. J. H.; Fuemmeler, E. G.; Feng, J.; Wu, J.; Greenham, N. C.; Chin, A. W.; Musser, A. J. Switching between Coherent and Incoherent Singlet Fission via Solvent-Induced Symmetry Breaking. *J Am Chem Soc* **2019**, *141* (44), 17558–17570. https://doi.org/10.1021/jacs.9b05561.
(35) Korovina, N. V.; Pompetti, N. F.; Johnson, J. C. Lessons from Intramolecular Singlet Fission with Covalently Bound Chromophores. *J Chem Phys* **2020**, *152* (4), 040904. https://doi.org/10.1063/1.5135307.
(36) Müller, S.; Heinze, J. Fluorescence Analysis of Two New TICT Systems: 10-Cyano-9,9′-Bianthryl (CBA) and 10, 10′-Dicyano-9,9′-Bianthryl (DCBA). *Chem Phys* **1991**, *157* (1–2), 231–242. https://doi.org/10.1016/0301-0104(91)87147-n.
(37) Jurczok, M.; Plaza, P.; Martin, M. M.; Meyer, Y. H.; Rettig, W. Excited State Relaxation Paths in 9,9′-Bianthryl and 9-Carbazolyl-Anthracene: A Sub-Ps Transient Absorption Study. *Chem Phys* **2000**, *253* (2–3), 339–349. https://doi.org/10.1016/s0301-0104(99)00386-9.
(38) Khara, D. C.; Paul, A.; Santhosh, K.; Samanta, A. Excited State Dynamics of 9,9′-Bianthryl in Room Temperature Ionic Liquids as Revealed by Picosecond Time-Resolved Fluorescence Study. *J Chem Sci* **2009**, *121* (3), 309–315. https://doi.org/10.1007/s12039-009-0035-6.
(39) Hashimoto, S.; Yabushita, A.; Kobayashi, T.; Okamura, K.; Iwakura, I. Direct Observation of the Change in Transient Molecular Structure of 9,9′-Bianthryl Using a 10 fs Pulse UV Laser.

Chem Phys **2018**, *512* (Bull. Chem. Soc. J. 49 4 1976), 128–134. https://doi.org/10.1016/j.chemphys.2017.12.016.
(40) Piet, J. J.; Schuddeboom, W.; Wegewijs, B. R.; Grozema, F. C.; Warman, J. M. Symmetry Breaking in the Relaxed S 1 Excited State of Bianthryl Derivatives in Weakly Polar Solvents. *J Am Chem Soc* **2001**, *123* (22), 5337–5347. https://doi.org/10.1021/ja004341o.
(41) Lee, C.; Choi, C. H.; Joo, T. A Solvent–Solute Cooperative Mechanism for Symmetry-Breaking Charge Transfer. *Phys Chem Chem Phys* **2019**, *22* (3), 1115–1121. https://doi.org/10.1039/c9cp05090f.
(42) Takaya, T.; Hamaguchi, H.; Iwata, K. Femtosecond Time-Resolved Absorption Anisotropy Spectroscopy on 9,9′-Bianthryl: Detection of Partial Intramolecular Charge Transfer in Polar and Nonpolar Solvents. *J Chem Phys* **2009**, *130* (1), 014501. https://doi.org/10.1063/1.3043368.
(43) Fujiwara, T.; Egashira, K.; Ohshima, Y.; Kajimoto, O. Effects of a Solvent Molecule on the Torsional Potential of 9,9′-Bianthryl. *Phys Chem Chem Phys* **2000**, *2* (7), 1365–1373. https://doi.org/10.1039/a910327i.
(44) Asami, N.; Takaya, T.; Yabumoto, S.; Shigeto, S.; Hamaguchi, H.; Iwata, K. Two Different Charge Transfer States of Photoexcited 9,9′-Bianthryl in Polar and Nonpolar Solvents Characterized by Nanosecond Time-Resolved Near-IR Spectroscopy in the 4500-10 500 Cm -1 Region. *J Phys Chem* **2010**, *114* (22), 6351–6355. https://doi.org/10.1021/jp912173h.
(45) Aster, A.; Licari, G.; Zinna, F.; Brun, E.; Kumpulainen, T.; Tajkhorshid, E.; Lacour, J.; Vauthey, E. Tuning Symmetry Breaking Charge Separation in Perylene Bichromophores by Conformational Control. *Chem Sci* **2019**, *10* (45), 10629–10639. https://doi.org/10.1039/c9sc03913a.
(46) Cook, R. E.; Phelan, B. T.; Kamire, R. J.; Majewski, M. B.; Young, R. M.; Wasielewski, M. R. Excimer Formation and Symmetry-Breaking Charge Transfer in Cofacial Perylene Dimers. *J Phys Chem* **2017**, *121* (8), 1607–1615. https://doi.org/10.1021/acs.jpca.6b12644.
(47) Dereka, B.; Koch, M.; Vauthey, E. Looking at Photoinduced Charge Transfer Processes in the IR: Answers to Several Long-Standing Questions. *Accounts Chem Res* **2017**. https://doi.org/10.1021/acs.accounts.6b00538.
(48) Loudet, A.; Burgess, K. BODIPY Dyes and Their Derivatives: Syntheses and Spectroscopic Properties. *Chem Rev* **2007**, *107* (11), 4891–4932. https://doi.org/10.1021/cr078381n.
(49) Nepomnyashchii, A. B.; Bard, A. J. Electrochemistry and Electrogenerated Chemiluminescence of BODIPY Dyes. *Accounts Chem Res* **2012**, *45* (11), 1844–1853. https://doi.org/10.1021/ar200278b.
(50) Golden, J. H.; Estergreen, L.; Porter, T.; Tadle, A. C.; R, D. S. M.; Facendola, J. W.; Kubiak, C. P.; Bradforth, S. E.; Thompson, M. E. Symmetry-Breaking Charge Transfer in Boron Dipyridylmethene (DIPYR) Dimers. *Acs Appl Energy Mater* **2018**, *1* (3), 1083–1095. https://doi.org/10.1021/acsaem.7b00214.
(51) Bartynski, A. N.; Gruber, M.; Das, S.; Rangan, S.; Mollinger, S.; Trinh, C.; Bradforth, S. E.; Vandewal, K.; Salleo, A.; Bartynski, R. A.; Bruetting, W.; Thompson, M. E. Symmetry-Breaking Charge Transfer in a Zinc Chlorodipyrrin Acceptor for High Open Circuit Voltage Organic Photovoltaics. *J Am Chem Soc* **2015**, *137* (16), 5397–5405. https://doi.org/10.1021/jacs.5b00146.
(52) Trinh, C.; Kirlikovali, K.; Das, S.; Ener, M. E.; Gray, H. B.; Djurovich, P.; Bradforth, S. E.; Thompson, M. E. Symmetry-Breaking Charge Transfer of Visible Light Absorbing Systems: Zinc Dipyrrins. *J Phys Chem C* **2014**, *118* (38), 21834–21845. https://doi.org/10.1021/jp506855t.

(53) Marcus, R. A. ON THE THEORY OF ELECTROCHEMICAL AND CHEMICAL ELECTRON TRANSFER PROCESSES. *Can J Chem* **1959**, *37* (1), 155–163. https://doi.org/10.1139/v59-022.
(54) Noginov, M. A.; Dewar, G.; McCall, M. W.; Zheludev, N. I.; Andrews, D. Tutorials in Complex Photonic Media. **2009**, 439–478. https://doi.org/10.1117/3.832717.ch14.
(55) Closs, G. L.; Calcaterra, L. T.; Green, N. J.; Penfield, K. W.; Miller, J. R. Distance, Stereoelectronic Effects, and the Marcus Inverted Region in Intramolecular Electron Transfer in Organic Radical Anions. *J Phys Chem* **1986**, *90* (16), 3673–3683. https://doi.org/10.1021/j100407a039.
(56) CLOSS, G. L.; MILLER, J. R. Intramolecular Long-Distance Electron Transfer in Organic Molecules. *Science* **1988**, *240* (4851), 440–447. https://doi.org/10.1126/science.240.4851.440.
(57) Young, R. M.; Wasielewski, M. R. Mixed Electronic States in Molecular Dimers: Connecting Singlet Fission, Excimer Formation, and Symmetry-Breaking Charge Transfer. *Accounts Chem Res* **2020**, *53* (9), 1957-1968. https://doi.org/10.1021/acs.accounts.0c00397.